http://dx.doi.org/10.5012/bkcs.2012.33.11.3805

Molecular Dynamics Simulation of a Small Drop of Liquid Argon

Song Hi Lee

Department of Chemistry, Kyungsung University, Busan 608-736, Korea. E-mail: shlee@ks.ac.kr
Received July 20, 2012, Accepted August 31, 2012

Results for molecular dynamics simulation method of small liquid drops of argon (N = 1200-14400 molecules) at 94.4 K through a Lennard-Jones intermolecular potential are presented in this paper as a preliminary study of drop systems. We have calculated the density profiles $\rho(r)$, and from which the liquid and gas densities ρ_l and ρ_g, the position of the Gibbs' dividing surface R_o, the thickness of the interface *d*, and the radius of equimolar surface R_e can be obtained. Next we have calculated the normal and transverse pressure tensor $p_N(r)$ and $p_T(r)$ using Irving-Kirkwood method, and from which the liquid and gas pressures p_l and p_g, the surface tension γ_s, the surface of tension R_s, and Tolman's length δ can be obtained. The variation of these properties with N is applied for the validity of Laplace's equation for the pressure change and Tolman's equation for the effect of curvature on surface tension through two routes, thermodynamic and mechanical.

Key Words : Drop of liquid argon, Irving-Kirkwood pressure, Surface tension, Molecular dynamics simulation

Introduction

The investigation of mechanical or thermodynamic properties of small systems is of great scientific and practical interest. When considering liquid drops in the theory of surface phenomena, a most important effect is the dependence of the surface tension on the drop size. The thermodynamic analysis of Gibbs[1] and the older mechanical ideas of Young, Laplace, and others[2-7] lead to several widely used formulas for droplets.

Laplace[2] considered a liquid droplet floating in a vapor phase and noticed that the surface tension of the liquid-vapor interface tries to contract the spherical surface of the droplet. The droplet must therefore be stabilized by a pressure difference over the interface that balances the contracting force. The Laplace equation expresses this condition for mechanical equilibrium for a three dimensional fluid:

$$\Delta p = \frac{2\gamma_s}{R_s}, \tag{1}$$

where $\Delta p = p_l - p_g$ is the pressure difference between the interior of the drop (p_l) and the gas (p_g) and γ_s is the surface tension referred to the surface of tension R_s (radius of tension).

The Tolman equation for the variation of the surface tension with drop size is given by

$$\frac{\gamma_s}{\gamma_\infty} = 1 - \frac{2\delta}{R_s} + \cdots, \tag{2}$$

where γ_∞ is the surface tension for the planar interface and $\delta = R_e - R_s$ is called Tolman's length after Tolman[3] with R_e the radius for the equimolar surface. Using Eqs. (1) and (2), the thermodynamic route leads to

$$R_s = \frac{3 - [9 - 4R_e {}^{\Delta p}/_{\gamma_\infty}]^{1/2}}{{}^{\Delta p}/_{\gamma_\infty}}. \tag{3}$$

The equimolar dividing surface at radius R_e is defined so that the system would contain an equal number of molecules where the density remains constant at its two respective limiting value on either side of the surface, with a discontinuous change at the surface itself. For a spherical drop, R_e is given by

$$R_e^3 = \frac{1}{\rho_g - \rho_l} \int_0^\infty dr\, r^3 \frac{d\rho(r)}{dr}. \tag{4}$$

The local pressure tensor $\boldsymbol{p}(r)$ for drops can be defined[8,9] in terms of the pair-correlation function of the fluid and although this definition is not unique, all tensors have in common that they satisfy the condition

$$\nabla \cdot \boldsymbol{p}(r) = 0 \tag{5}$$

in the absence of an external filed. Furthermore, all tensors become isotropic in a bulk phase with diagonal components p, the pressure in the bulk. In a spherical symmetry, the pressure tensor has only two independent components

$$\boldsymbol{p}(r) = p_N(r)\hat{\mathbf{r}}\hat{\mathbf{r}} + p_T(r)(I - \hat{\mathbf{r}}\hat{\mathbf{r}}) \tag{6}$$

where $\hat{\mathbf{r}}$ is a unit vector in the direction **r**, **r** is the distance from the origin, and I is the unit tensor. $p_N(r)$ and $p_T(r)$ are the normal and transverse components of the pressure tensor at position **r**, respectively.

The general condition of mechanical equilibrium, Eq. (5), leads to

$$\frac{dp_N(r)}{dr} = -\frac{2}{r}[p_N(r) - p_T(r)]. \tag{7}$$

Note that $p_N(r)$ and $p_T(r)$ both become equal to the bulk pressure p in a bulk phase. Integrating Eq. (7) from 0 to a position R_v (or ∞) sufficiently deep in the vapor phase gives the pressure difference Δp,

$$\Delta p = 2\int_0^\infty dr \frac{1}{r}[p_N(r) - p_T(r)]. \tag{8}$$

Combining to the Laplace Eq. (1), we obtain for the surface tension

$$\gamma_s = \int_0^\infty dr \frac{R_s}{r}[p_N(r) - p_T(r)] . \quad (9)$$

From mechanical arguments for the force and torque on a hypothetical strip cutting the surface of the drop, Bakker[10] and Buff[11] obtained the equation

$$\gamma_s = \int_0^\infty dr \left(\frac{r}{R_s}\right)^2 [p_N(r) - p_T(r)] . \quad (10)$$

Eq. (9) is invariant to the form of the pressure tensor, whereas Eq. (10) is not. Combining Eqs. (7) and (10), using Eq.(1), gives for γ_s

$$\gamma_s^3 = -\frac{1}{8}(p_l - p_g)^2 \int_0^\infty dr\ r^3 \frac{dp_N(r)}{dr} . \quad (11)$$

Molecular Dynamics Simulation and Irving-Kirkwood Pressure Tensor. The usual Lennard-Jones (LJ) 12-6 potential for the interaction between argon molecules is used with LJ parameters, $\sigma = 0.34$ nm and $\varepsilon/k_B = 120$ K, where k_B is the Boltzmann constant. The inter-atomic potential is truncated at $r_c = 4\sigma$ and long-range corrections are applied to the energy, pressure, *etc.* due to the potential truncation.[12] The time integrations for the equation of translational motion is solved using the velocity-Verlet algorithm[13] with a time step of 5×10^{-15} second (5 fs). The temperature (94.4 K) is kept constant by using a Nose-Hoover[14,15] thermostat. These systems of N = 1200, 1800, 3600, 7200, 10800, and 14400 molecules of argon are fully equilibrated in cubic boxes with spherical boundary conditions[16]:

$$u_k = k(r_i - r_o)^2, \quad r_i > r_o$$
$$= 0, \qquad r_i < r_o \quad (12)$$

where $k = 25$ cal/mol and r_o is given in Table 1 for each system of N. This external repulsive potential serves to prevent molecules from leaving the spherical cell. The values of k and r_o have to be chosen with care. The value of r_o must not be so small that the potential interferes the drop, nor so large that the vapor phase is very large or that the drop evaporates.

The Irving-Kirkwood (IK) pressure tensor is calculated by an extension to a spherically symmetric system of the method described by Tsai.[17] Details of the calculation of $p_N^{IK}(r)$ is are given in the appendix of Ref. 16 and we describe the brief calculation here. The normal component $p_N(r)$ is the sum of kinetic and configurational terms

$$p_N(r) = p_K(r) + p_U(r) , \quad (13)$$

where $p_K(r) = k_B T\rho(r)$ is the kinetic term. The configurational term is given by

$$p_U(r) = S^{-1} \Sigma_k f_k , \quad (14)$$

where $S = 4\pi r^2$ is the area of a spherical surface of radius r and the sum over k is over the normal components of all the pair forces f_k acting across the surface. For a single surface S and one pair of molecules, the relevant geometry is given in Figure 1. Depending on the location of molecule i and j, the force acts across no [Fig. 1(a)], only one [Fig. 1(b)], or two intersection(s) [Fig. 1(c)]. The force vector $\mathbf{f}(r_{ij})$ is given by

$$\mathbf{f}(r_{ij}) = \hat{\mathbf{r}}_{ij} f(r_{ij}) = -\hat{\mathbf{r}}_{ij} \frac{du(r_{ij})}{dr_{ij}} \text{ and } f_k = |\hat{\mathbf{r}} \cdot \hat{\mathbf{r}}_{ij}| f(r_{ij}) = |\mathbf{r} \cdot \mathbf{r}_{ij}| f(r_{ij})/r r_{ij}$$

so that

$$p_U(r) = -(4\pi r^3)^{-1} \Sigma_k |\mathbf{r} \cdot \mathbf{r}_{ij}| \frac{1}{r_{ij}} \frac{du(r_{ij})}{dr_{ij}} . \quad (15)$$

Since the end of $\mathbf{r}$ ($\mathbf{r}_A$ or $\mathbf{r}_B$) lines on S and is between i and j, we can write in Figure 1(c)

$$\mathbf{r} = \frac{1}{2}(\mathbf{r}_i + \mathbf{r}_j) + \lambda \frac{1}{2}\mathbf{r}_{ij} , \quad (16)$$

where λ is an undetermined constant in the range $-1 \le \lambda \le 1$ so that $\mathbf{r} = \mathbf{r}_A$, $\lambda < 0$ and $\mathbf{r} = \mathbf{r}_B$, $\lambda > 0$. We can find the two λ values for $\mathbf{r}_A$ and $\mathbf{r}_B$ for a given surface, λ_+ and λ_-, so that the f_k acts across the surface by squatting Eq. (16) and solving the resulting quadratic:

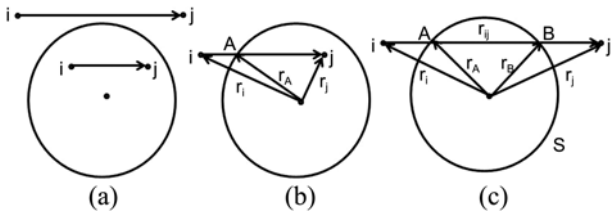

Figure 1. Geometry for calculating the contribution to the pressure tensor from a pair of molecules i and j with (a) no, (b) only one, (c) or two intersection(s).

Table 1. The parameter of external repulsive potential in Eq. (12) r_o, the liquid and gas densities ρ_l and ρ_g, the position of the Gibbs' dividing surface R_o, the thickness of the interface d, the radius of equimolar surface R_e, number of molecules in the drop N_d, and the percentage of N_d/N obtained from this work

N	r_o (nm)	ρ_l (g/cm^3)	ρ_g (g/cm^3)	R_o (nm)	d (nm)	R_e (nm)	N_d	N_d/N (%)
14400	10.99	1.360	0.008	5.47	0.77	5.48	13985	97.1
10800	9.99	1.364	0.010	4.96	0.80	4.99	10464	96.9
7200	8.72	1.365	0.014	4.31	0.79	4.34	6910	96.0
3600	6.92	1.371	0.020	3.38	0.80	3.43	3375	93.8
1800	5.50	1.384	0.031	2.40	0.76	2.45	1625	90.2
1200	4.80	1.403	0.044	2.02	0.80	2.08	1033	86.1

$$\lambda_{\pm} = \frac{r_i^2 - r_j^2}{r_{ij}^2} \pm \left[\left(\frac{r_i^2 - r_j^2}{r_{ij}^2} \right)^2 + 1 - \left(\frac{r_i^2 - r_j^2}{r_{ij}^2} \right) + \frac{4r^2}{r_{ij}^2} \right]^{1/2} \quad (17)$$

and so for both intersection the scalar product that appears in Eq. (15) has the same value as required by symmetry. The final result is obtained from **r** in Eq. (17):

$$|\mathbf{r} \cdot \mathbf{r}_{ij}| = \frac{1}{2} r_{ij}^2 \left[\left(\frac{r_i^2 - r_j^2}{r_{ij}^2} \right)^2 + 1 - \left(\frac{r_i^2 - r_j^2}{r_{ij}^2} \right) + \frac{4r^2}{r_{ij}^2} \right]^{1/2} . \quad (18)$$

If both $|\lambda_+| \le 1$ and $|\lambda_-| \le 1$, there are two intersection [Fig. 1(c)]. If both $|\lambda_+| > 1$ and $|\lambda_-| > 1$, there is no intersection [Fig. 1(a)]. For the other cases, there is only one interaction [Fig. 1(b)]. The following two equalities are used: $(\mathbf{r}_i + \mathbf{r}_j) \cdot \mathbf{r}_{ij} = r_j^2 - r_i^2$ and $2\mathbf{r}_i \cdot \mathbf{r}_j = r_i^2 + r_j^2 - r_{ij}^2$.

Results and Discussion

Typical density profiles for different numbers of argon molecules (N), obtained from simulations, are shown in Figure 2 as dashed lines. A hyperbolic tangent function of the form[18]

$$\rho(r) = \frac{1}{2}(\rho_l + \rho_g) - \frac{1}{2}(\rho_l - \rho_g) \tanh[2(r - R_o)/d] \quad (19)$$

is fitted to the simulation results where R_o is the position of the Gibbs' dividing surface and *d* is a parameter for thickness of the interface. In the drop center the counting statistics are so poor because of the low volume of each shell in this region that the density profile of the central part is artificially flat. The fitted $\rho(r)$ and the positions of R_o are shown as solid lines and as dotted lines in Figure 2, respectively. The values of R_o and *d* used in Eq. (19) with ρ_l and ρ_g are given in Table 1 for different numbers of argon molecules (N). Both densities strongly increase with decreasing N. Using Eq. (4) and the obtained density profiles $\rho(r)$, the radii R_e for the equimolar surface for different numbers of argon molecules (N) are calculated and also listed in Table 1. The values for R_o and R_e are very close each other and they increase with increasing N.

To estimate a measure of the average drop size, the number of molecules N_d in the drop is defined as[16]

$$N_d = 4\pi \int_0^{R_{10}} dr\, r^2 \rho(r) , \quad (20)$$

where

$$\rho(R_{10}) = \rho_g + 0.10(\rho_l - \rho_g) . \quad (21)$$

The drop contains molecules out to a radius R_{10} where the local density has fallen to the gas density plus 10% of the difference between ρ_l and ρ_g. The values of N_d obtained from the simulation are listed in Table 1. The percentage of N_d/N (Table 1) strongly decreases with decreasing N, in accord with the strong increment of ρ_g with decreasing N, indicating that small drops are only stable in surroundings of a high pressure gas phase. Or it might be related to artificially the volume of the cubic simulation box in which the drop of liquid argon is immersed.

Figures 3 and 4 show the normal and transverse components of the pressure tensor. First, $p_N^{IK}(r)$ are obtained from the simulation according to the Irving-Kirkwood (IK) method, Eqs. (13)-(18), and then $p_T^{IK}(r)$ are derived from these by Eq. (7). The central part of the kinetic term $p_T^{IK}(r)$ in Eq. (13) is flat because of poor statistics for $\rho(r)$ in the drop center, while the configurational term $p_U^{IK}(r)$ is not since many pairs of molecules *i* and *j* give contribution to the pressure tensor in the drop center. The central part of the

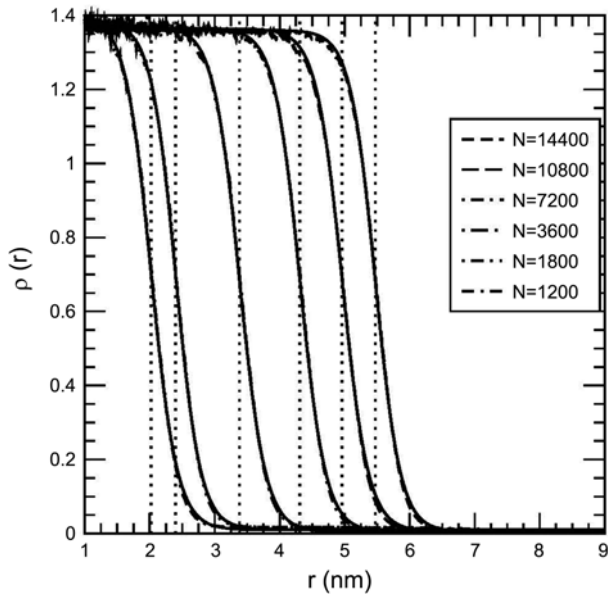

Figure 2. Density profiles for different numbers of argon molecules (N) at 94.4 K, obtained from simulations, are shown as dashed lines. The fitted $\rho(r)$ as Eq. (19) are shown as solid lines and the straight dotted lines represent the positions of R_o.

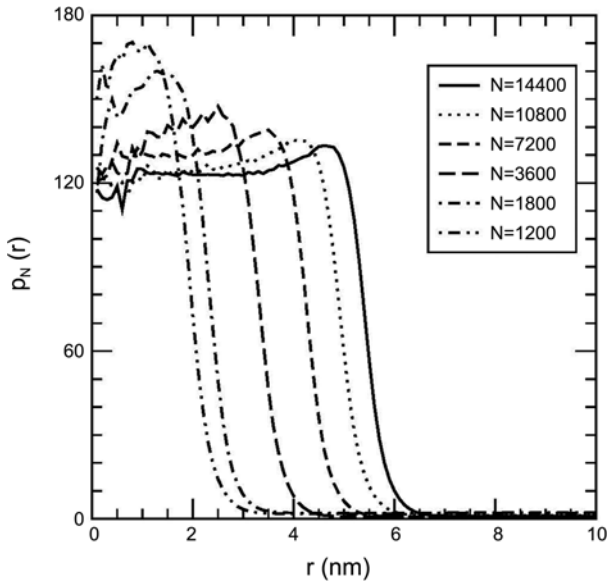

Figure 3. The Irving-Kirkwood (IK) normal pressure tensor at 94.4 K.

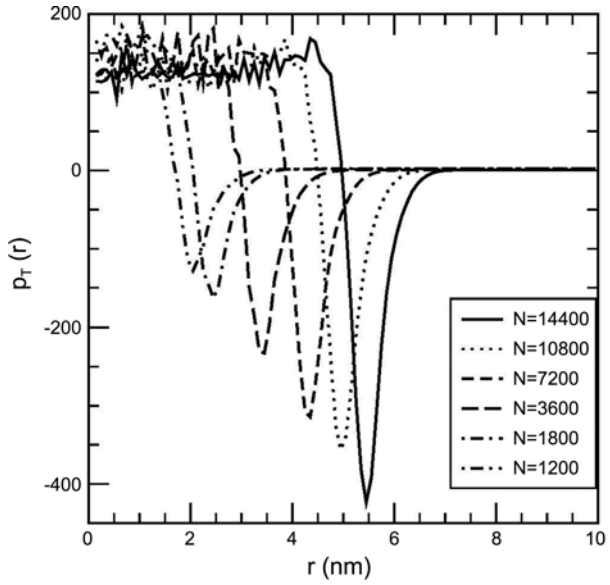

Figure 4. The Irving-Kirkwood (IK) transverse pressure tensor at 94.4 K.

final $p_N^{IK}(r)$ is not flat unlike the earlier study.[16] It increases with r and decreases after a maximum at $r_{max} < R_e$.

The values of p_l and p_g in Table 2 are obtained by averaging $p_N^{IK}(r)$ from r = 0 to r_{max} and from $r = R_e+d/2$ to $r = \infty$, respectively, instead of using Eq. (19) with ρ replaced by p_N^{IK} as reported in Ref. 16. Both p_l and p_g decrease with increasing N indicating high p_l and p_g at small N. The value of $\Delta p = p_l - p_g$ may be different from $\Delta p = p_N^{IK}(0) - p_N^{IK}(\infty)$ which is obtained from Eqs. (7) and (8). The values of $\frac{\Delta p}{\gamma_\infty}$ in Eq. (3) with $\gamma_\infty = 10.77$ mN/m[19] ranged in 1.1-1.5 nm^{-1} are normal but R_e in Table 1 are large, which results in $4R_e\frac{\Delta p}{\gamma_\infty} > 9$ for all the cases of N. This concludes that Eq. (3), the thermodynamic route, is unable to calculate R_s. The criterion for the thermodynamic route, $R_e\frac{\Delta p}{\gamma_\infty} < 9/4$, is somewhat irrational since R_e increases with increasing N as seen in Table 1, showing that Eq. (3) is unsuccessful for large R_e and therefore for large N.

The mechanical route for γ_s, Eq. (10), has an analogy to γ_∞ for the planar interface:

$$\gamma_\infty = \frac{1}{2}\int_0^\infty dz[p_N(z) - p_T(z)] = \frac{1}{2}L_z[\bar{p}_N - \bar{p}_T], \qquad (22)$$

where $p_N(z)$ and $p_T(z)$ are the normal and transverse components of the pressure tensor at position z, respectively, with L_z the length of z-side of simulation box. Recent studies for vapor-liquid interface at 94.4 K using a test-area molecular dynamics simulation method have reported an excellent agreement with the experimental data for γ_∞.[20,21]

The values of the surface tension γ_s using Eq. (11), the mechanical route plus the Laplace equation, obtained from the simulation are listed in Table 2 for different numbers of argon molecules (N). γ_s increases with increasing N, and gives the exact value of γ_∞ for N = 3600 so that Tolman's length δ in this case is 0 according to Eq. (2). Generally γ_s is less than γ_∞ due to $\delta > 0$ [Eq. (2)], but γ_s obtained from simulations are larger than γ_∞ for N > 7200. This is also reported in the other study. For example, γ_s^* is 0.85 for the thermodynamics route and 0.74 for the mechanical route in the case of N = 2048 (the largest N in Ref. 16) with $\gamma_\infty^* = 0.75$ where the reduced γ^* is defined as $\gamma\frac{\sigma^2}{\varepsilon}$. This indicates that the liquid drops of argon in this study are somewhat large.

The values of R_s and δ, calculated from the values of γ_s using Eqs. (1) and (2), are listed in Table 2. The results from Eq. (1) are reasonable, while those from Eq. (2) are somewhat unacceptable except the cases of small N. The Tolman's lengths are negative for large N. The failure of the thermodynamic route for R_s, Eq. (3), is originated from the Tolman equation, Eq. (2), for large N. Note that the Laplace equation, Eq. (1), $\gamma_s = \frac{1}{2}R_s \cdot \Delta p$ is very similar to Eq. (22) for γ_∞.

In summary, we have carried out molecular dynamics simulations of small liquid drops of argon (1200-14400 molecules) at T = 94.4 K in which the atoms interact with a Lennard-Jones intermolecular potential cutoff at 4σ with spherical boundary conditions. The obtained surface tension γ_s using the mechanical route increases with increasing N, and gives the exact value of γ_∞ (surface tension for the planar interface) for N = 3600 so that Tolman's length δ = 0 in this case. Generally γ_s is less than γ_∞ due to $\delta > 0$ (the Tolman equation), but γ_s obtained from simulations are larger than γ_∞ for N > 7200. The thermodynamic route, combining the Laplace equation and the Tolman equation, is failed for large radii of the equimolar surface R_e and therefore for large N which is originated from the Tolman equation for large N. This result restricts the size of liquid drop of argon to be less than N = 3600.

Acknowledgments. This research was supported by

Table 2. The liquid and gas pressures ρ_l and ρ_g, the surface tension γ_s, the surface of tension R_s, and Tolman's length δ obtained form this work

N	ρ_l (bar)	ρ_g (bar)	γ_s (mN/m)	R_s (nm), Eq. (1)	δ (nm), Eq. (1)	R_s, Eq. (2)	δ, Eq. (2)
14400	123.5	1.1	15.8	2.58	2.90	7.15	-1.67
10800	125.1	1.2	14.6	2.36	2.63	6.07	-1.08
7200	131.0	1.3	13.3	2.05	2.29	4.92	-0.58
3600	135.1	1.6	10.8	1.62	1.81	3.43	0.00
1800	147.8	2.0	8.24	1.13	1.32	2.19	0.26
1200	163.8	2.1	6.47	0.80	1.28	1.73	0.35

Kyungsung University Research Grants in 2012.

References

1. Gibbs, G. W. *Collected Works*; Yale Univ. Press: New Haven, 1948, Vol. 1.
2. Rowlinson, J. S.; Widom, B. *Theory of Capillarity*; Oxford: Clarendon: 1982.
3. Tolman, R. C. *J. Chem. Phys*. **1949**, *17*, 333.
4. Koenig, F. O. *J. Chem. Phys*. **1950**, *18*, 449.
5. Buff, F. P. *J. Chem. Phys*. **1951**, *19*, 1591.
6. Hill, T. L. *J. Phys*. *Chem.* **1952**, *56*, 526.
7. Kond, S. *J. Chem. Phys*. **1956**, *25*, 662.
8. Schofield, D.; Henderson, J. R. *Proc. R. Soc. London* **1982**, *Ser. A 379*, 231.
9. Baus, M.; Lovett, R. *Phys. Rev. Lett*. **1990**, *65*, 1781.
10. Ono, S.; Kondo, S. In *Encyclopedia of Physics*; Flugge, S., Ed.; Springer: Berlin, 1960; Vol. 10, Sec. 37, p 134. In Sec. 15 they ascribe Eq. (9) to Bakker.
11. Buff, P. F. *J. Chem. Phys*. **1955**, *23*, 419.
12. Allen, M. P.; Tildesley, D. J. *Computer Simulation of Liquids*; Oxford Univ. Press: Oxford, 1987; p 64.
13. Swope, W. C.; Andersen, H. C.; Berens, P. H.; Wilson, K. R. *J. Chem. Phys*. **1982**, *76*, 637.
14. Hoover, W. G. *Phys. Rev. A* **1985**, *31*, 1695.
15. Nosé, S. *Mol. Phys*. **1984**, *52*, 255.
16. Thompson, S. M.; Gubbins, K. E.; Walton, J. P. R. B.; Chantry, R. A. R.; Rowlinson, J. S. *J. Chem. Phys*. **1984**, *81*, 530.
17. Tsai, D. H. *J. Chem. Phys.* **1978**, *70*, 1375.
18. Chapela, G. A.; Saville, G.; Thompson, S. M.; Rowlinson, J. S. *J. Chem. Soc. Faraday Trans. II* **1977**, *8*, 133.
19. NIST Chemistry WebBook. http://webbook.nist.gov/chemistry/fluid (accessed 2011).
20. Lee, S. H. *Bull. Kor. Chem. Soc*. **2012**, *33*, 167.
21. Lee, S. H. *Bull. Kor. Chem. Soc*. **2012**, *33*, 3039.